Heparan sulfate/heparin promotes transthyretin fibrillization through selective binding to a basic motif in the protein

Fredrik Noborn[a], Paul O'Callaghan[b,1], Erik Hermansson[c,1], Xiao Zhang[b], John B. Ancsin[a], Ana M. Damas[d], Ingrid Dacklin[e], Jenny Presto[c], Jan Johansson[c], Maria J. Saraiva[f], Erik Lundgren[e], Robert Kisilevsky[g], Per Westermark[h], and Jin-Ping Li[a,2]

[a]Department of Medical Biochemistry and Microbiology, The Biomedical Center, Uppsala University, Husargatan 3, Box 582, 751 23 Uppsala, Sweden; [b]Department of Public Health and Caring Sciences, Molecular Geriatrics, Rudbeck Laboratory, Uppsala University, Dag Hammarskjöldsväg 20, 751 85 Uppsala, Sweden; [c]Alzheimer's Disease Research Center, Department of Neurobiology, Care Sciences and Society, Karolinska Institutet, S-141 86 Stockholm, Sweden; [d]Molecular Structure Group, Instituto de Biologia Molecular e Celular, University of Porto, Rua do Campo Alegre, 823, 4150-180 Porto, Portugal; [e]Department of Molecular Biology, Umeå University, 901 87 Umeå, Sweden; [f]Molecular Neurobiology Group, Instituto de Biologia Molecular e Celular, University of Porto, Rua do Campo Alegre, 823, 4150-180 Porto, Portugal; [g]Department of Pathology and Molecular Medicine, Richardson Laboratory, 88 Stuart Street, Queen's University, Kingston, ON, Canada K7L 3N6; and [h]Department of Genetics and Pathology, Rudbeck Laboratory, Uppsala University, Dag Hammarskjöldsväg 20, 751 85 Uppsala, Sweden

Edited by Reed B. Wickner, National Institutes of Health, Bethesda, MD, and approved February 16, 2011 (received for review February 3, 2011)

Transthyretin (TTR) is a homotetrameric protein that transports thyroxine and retinol. Tetramer destabilization and misfolding of the released monomers result in TTR aggregation, leading to its deposition as amyloid primarily in the heart and peripheral nervous system. Over 100 mutations of TTR have been linked to familial forms of TTR amyloidosis. Considerable effort has been devoted to the study of TTR aggregation of these mutants, although the majority of TTR-related amyloidosis is represented by sporadic cases due to the aggregation and deposition of the otherwise stable wild-type (WT) protein. Heparan sulfate (HS) has been found as a pertinent component in a number of amyloid deposits, suggesting its participation in amyloidogenesis. This study aimed to investigate possible roles of HS in TTR aggregation. Examination of heart tissue from an elderly cardiomyopathic patient revealed substantial accumulation of HS associated with the TTR amyloid deposits. Studies demonstrated that heparin/HS promoted TTR fibrillization through selective interaction with a basic motif of TTR. The importance of HS for TTR fibrillization was illustrated in a cell model; TTR incubated with WT Chinese hamster ovary cells resulted in fibrillization of the protein, but not with HS-deficient cells (pgsD-677). The effect of heparin on TTR fibril formation was further demonstrated in a *Drosophila* model that overexpresses TTR. Heparin was colocalized with TTR deposits in the head of the flies reared on heparin-supplemented medium, whereas no heparin was detected in the nontreated flies. Heparin of low molecular weight (Klexane) did not demonstrate this effect.

systemic amyloidosis | sulfated glycosaminoglycans | aging | heart failure

Transthyretin (TTR) is a functional plasma protein composed of four 14-kDa subunits (1, 2). TTR is synthesized predominantly by the liver and functions as a transporter for retinol and thyroxine (3). In addition to its physiological functions, TTR is found as a main constituent of amyloid fibrils in several distinct clinical forms of amyloidoses, including familial amyloid polyneuropathy (4), familial cardiac amyloidosis (5) and sporadic senile systemic amyloidosis (SSA) (6). SSA is caused by the s elective deposition of wild-type (WT) TTR fibrils in cardiac tissue (7), affecting almost 25% of the population above 80 y of age (8, 9).

Around 100 amino acid mutations of TTR have been linked to familial forms of TTR amyloidoses (10). Studies have shown that TTR forms amyloid through a process that is initiated by tetramer destabilization. The destabilization results in accumulation of monomers, which can misfold and aggregate into fibrillar structures (11). Considerable effort has been devoted to studying the amyloidogenicity of TTR mutations related to the familial forms of the disease, though the majority of TTR-related amyloidosis is represented by sporadic cases caused by aggregation and deposition of the otherwise stable WT protein.

Heparan sulfate (HS), a sulfated polysaccharide consisting of repeating units of glucosamine and glucuronic acid, is associated with amyloid deposits in a number of amyloidoses (12–14). Although the precise role of HS in the pathology of amyloidosis remains unresolved, accumulating evidence suggests that HS plays an important part in amyloid deposition. Previously, we have demonstrated that amyloid A amyloidosis is correlated with HS chain length in a mouse model (15).

In the present work, we detected codeposition of HS with TTR in the cardiomyopathic heart by immunohistochemical stainings. In vitro studies revealed that HS and heparin promoted TTR fibrillogenesis, an effect that correlated with the degree of sulfation of the polysaccharide, and was exerted through a specific binding sequence on TTR. This promoting effect was further examined in a *Drosophila* model that expresses human TTR (16). Thus, interaction of TTR with heparin/HS is size-dependent and selective, with a preference for polysaccharides with higher degrees of sulfation.

Results

Codeposition of HS and TTR Amyloid in the Cardiomyopathic Heart. Congo red staining of 15-μm-thick sections of the heart from a patient diagnosed with cardiomyopathy revealed apple-green birefringence when viewed under polarized light (Fig. 1*A*), demonstrating amyloid deposition in the specimen. Sulfated Alcian blue staining of the adjacent section revealed a pattern that resembles the Congo red positive morphology (Fig. 1*B*). Double immunostaining confirmed that TTR deposition is largely colocalized with HS (Fig. 1 *C–E*). In comparison, staining of heart sections from an age-matched control did not produce immunosignals for TTR (Fig. 1*F*). The codeposition of TTR and HS was prominent in the extracellular space and appeared tightly associated with myocyte membranes, whereas the codeposition in the vasculature was more variable with some vessel walls lack-

Author contributions: F.N., J.B.A., E.L., R.K., and J.-P.L. designed research; F.N., P.O., E.H., X.Z., and I.D. performed research; A.M.D. and M.J.S. contributed new reagents/analytic tools; F.N., P.O., E.H., J.B.A., A.M.D., J.P., J.J., M.J.S., E.L., R.K., P.W., and J.-P.L. analyzed data; and F.N., P.O., R.K., and J.-P.L. wrote the paper.

The authors declare no conflict of interest.

This article is a PNAS Direct Submission.

[1]P. O. and E. H. contributed equally to this work.

[2]To whom correspondence should be addressed. E-mail: jin-ping.li@imbim.uu.se.

This article contains supporting information online at www.pnas.org/lookup/suppl/doi:10.1073/pnas.1101194108/-/DCSupplemental.

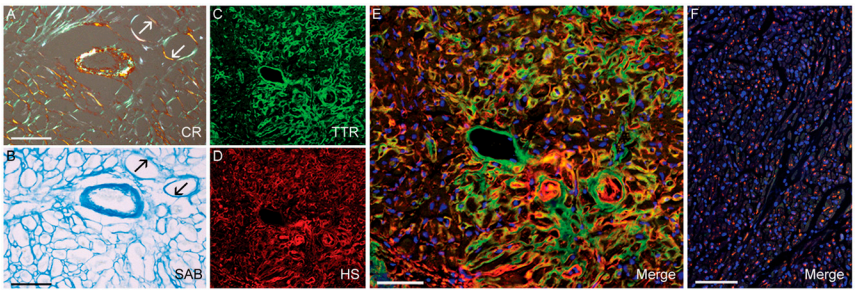

Fig. 1. Colocalization of TTR amyloid and HS in the heart of cardiomyopathy. Mycocardial sections (15 μm thick) from a 70-y-old patient with reported cardiomyopathy stained with Congo red were viewed under polarized light (*A*), and an adjacent section was stained with Alcian blue (*B*). Arrows in *A* and *B* indicate adjacent locations. Additional sections were double immunostained with antibodies against TTR (*C*, green) and HS (*D*, red). Merging the red and green fluorescent channels shows overlapped positive signals for TTR and HS in patient specimen (*E*) and negative staining of TTR in age-matched control subject (*F*). DAPI counterstaining for nuclei (blue). Original magnification, *A*–*F*, 200. Scale bar, 50 μM.

ing HS positive staining (Fig. 1 *C* and *E*). No TTR deposition or HS accumulation was detected in the control tissues (Fig. 1*F*).

Heparin and HS Promote Fibrillization of WT TTR. Thioflavin T (17) fluorescence analysis revealed that the recombinant human WT TTR expressed in a bacterial system exhibited low spontaneous fibrillization upon incubation at 37 °C for 48 h, even at low pH (2.7) condition (Fig. S1). However, addition of heparin (an analogue of HS) at this condition prompted TTR aggregation, forming substantial amounts of amyloid-like fibrils (Fig. 2*A*). Incubation of TTR with heparin-derived oligomers revealed a size dependence effect of heparin, as fragments (12-mer and 6-mer) less than 18-sugar residues had considerably lower effects than longer polymers. Notably, TTR incubated with an 18-mer resulted in more amyloid-like fibrils compared to the TTR incubation with full-length heparin (approximately 50-mer). HS with higher degrees of sulfation (HS II) enhanced the fibrillization of TTR effectively, albeit to a lesser degree compared to heparin, whereas low sulfated HS (HS I) had a marginal effect on TTR aggregation (Fig. 2*B*).

Analysis of the TTR incubated with or without heparin by native PAGE showed that the TTR–heparin aggregate displayed a different migration pattern. In contrast to the continuous smear appearance of the TTR aggregates without heparin, coincubation with heparin resulted in substantial macromolecular TTR aggregates migrating in the top of the gel, apart from the nonaggregated band observed prior to incubation, representing mono-, di-, and tetramers (Fig. 2*C*). This effect of heparin on TTR aggregation is more pronounced at higher concentrations, suggesting a dose-dependent effect. The TTR–heparin incubation generated Congo red positive fibrils as visualized under fluorescence and polarized light microscopy (Fig. 2*D*), whereas the TTR incubated without heparin was Congo red negative.

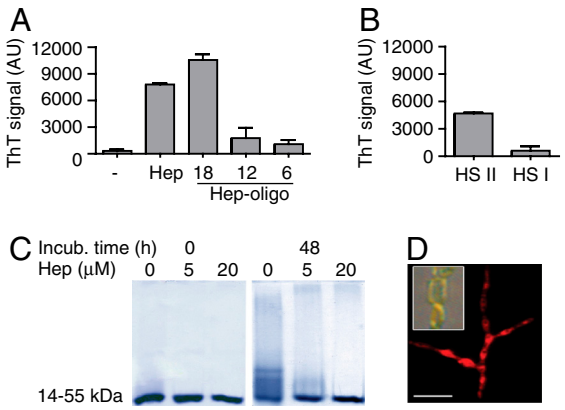

Fig. 2. Effect of heparin and HS on WT TTR aggregation. (*A* and *B*) The TTR dissolved in phosphate buffer (50 μM, pH 2.7) was incubated alone or with different heparin or HS (12 μM) at 37 °C for 48 h. After incubation, the samples were mixed with ThT and fluorescence was measured (see *Materials and Methods*). Data shown represent triplicate experiments (means ± SEM). (*C*) TTR (500 μM) incubated with heparin (0, 5, or 20 μM) under the same conditions were analyzed with native PAGE as described in *Materials and Methods*. The gel shows a different migration pattern of TTR incubated with or without heparin. The fibrils migrated in the stacking gel are not shown. (*D*) Microscopic analysis of the TTR after incubation with heparin. The sample was spotted on a glass and stained with Congo red. Images were taken under fluorescent light (original magnification, 20×. Scale bar, 5 μm) and polarized light (*Inset*).

To determine whether heparin was integrated/cofibrillized into the resulting TTR fibrils or only acted as a catalyst for the fibrillogenesis, TTR was incubated with a mixture of ^{3}H-labeled and unlabeled heparin. The samples of coincubated heparin-TTR and heparin alone were separated on native PAGE. Alcian blue staining visualized a heparin migration pattern that was indistinguishable between the two samples (Fig. 3*A*). Analysis of ^{3}H-labeled heparin by counting the radioactivity in the gel sections (cut as illustrated in Fig. 3*A*) show that heparin incubated alone was mainly recovered in sections 4, 5, and 6 (Fig. 3*B*), in accord with the Alcian blue staining. In contrast, heparin coincubated with TTR was substantially recovered in section 1 (the stacking section), in addition to sections 4, 5, and 6. Notably, Alcian blue failed to stain the heparin in section 1 for the heparin-TTR coincubated sample, possibly due to a masking effect by the resulting TTR amyloid-like fibrils.

To verify that the heparin recovered in section 1 is not a result of heparin interacting with aggregated TTR, ^{3}H-labeled heparin was incubated with preaggregated TTR. Analysis of the product by the same method showed a distribution pattern of ^{3}H-labeled heparin (Fig. S2) that it is almost identical to that of heparin alone (Fig. 3*B*), indicating that no or very little heparin interacted with aggregated TTR.

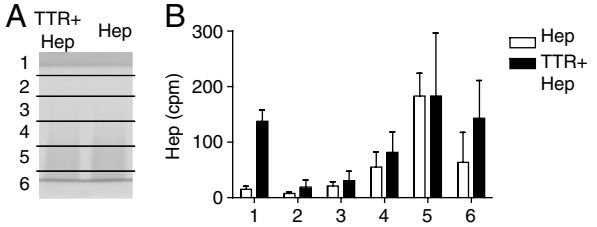

Fig. 3. Heparin integration into TTR fibrils. TTR dissolved in phosphate buffer (pH 2.7) was coincubated with heparin (mixture of ^{3}H-labeled and unlabeled) at 37 °C for 48 h. (*A*) The TTR–heparin coincubated sample and heparin alone were separated with native PAGE and stained with Alcian blue. (*B*) An identical set of samples was separated on the native PAGE as above, and each lane was cut into six sections (as illustrated in *A*). The gel slices were incubated for 2 h in H_2O to extract the heparin. The radioactivity was measured by scintillation counting.

Characterization of TTR–Heparin/HS Interaction. To further investigate the mechanism for the TTR–heparin/HS interaction, we applied surface plasmon resonance (SPR) spectroscopy. Dissociated TTR was immobilized onto a Biacore sensor chip, and heparin was allowed to interact with the ligand at neutral (pH 7.4) and mildly acidic (pH 5.0) conditions. Heparin binding to dissociated TTR was observed in mildly acidic pH, but not in the neutral condition, demonstrating a pH dependency for the interaction (Fig. 4*A*). The pH-dependent interaction was also observed for HS II (an HS species with higher sulfation degree) that displayed substantial binding at pH 5.0, but significantly reduced binding at pH 5.5 (Fig. 4*B*). The SPR spectroscopy analysis also showed that sulfation degree of HS/heparin plays a role in this interaction, as affinity of TTR for heparin is 10-fold higher than for HS II, and more than 1,000-fold higher than for the low sulfated HS I (Fig. S3 *A–C*). This pH- and sulfation degree–dependent interaction was further confirmed by measuring fibril formation of TTR incubated with heparin and HS II at pH 5.0 and 7.4 for 7 d (Fig. 4*C*).

To characterize the TTR–heparin interaction, we incubated TTR and its peptide fragments with ^{3}H-heparin. The binding was analyzed by a nitrocellulose-filter trapping method (18). Among the 16 peptides tested, only the peptide of aa 24-35 (PAINVAVHVFRK) bound to heparin (Fig. 5*B*). This heparin-binding peptide contains three basic amino acids, including a histidine that likely contributed to the pH dependency seen in the TTR–heparin/HS interaction. This selective binding property was further verified by SPR analysis (Fig. S4). The 24-35 peptide containing the V30M mutation, which is associated with familial amyloid neuropathy, showed substantially lower binding to heparin compared to the WT peptide (Fig. 5*B*).

From the binding assay, we noticed that heparin preferentially bound to dissociated TTR (Fig. 5*B*). For verification, we immobilized the dissociated and native TTR on to Biacore chips and injected HS II over the surface at pH 5.0. The obtained sensorgrams revealed stronger binding of HS II to dissociated TTR (Fig. S5). These results suggest that the heparin/HS binding domain of TTR is cryptic in the natively folded protein.

HS/Heparin Promotes Fibrillization of TTR in Cell Culture and in Vivo. To investigate whether the effect of HS/heparin in TTR fibrillization is also applicable to cells, the dissociated TTR was incubated with cultures of Chinese hamster ovary WT (CHO-WT) and HS-deficient (CHO-pgsD-677) cells (19) for 48 h. After incubation, the cells were washed extensively in PBS to remove free TTR. ThT fluorescence analysis of the cell lysates revealed substantial amounts of amyloid-like fibrils in the CHO-WT cells compared to that in the HS-deficient CHO-pgsD-677 cells (Fig. S6*A*), demonstrating an effect of HS on TTR fibrillization. Immunocytostaining of the cells with anti-TTR antibody detected trace amounts of positive immunosignals in the HS-deficient cells (CHO-pgsD-677); in comparison, strong positive signals were found in CHO-WT cells (Fig. S6*B*).

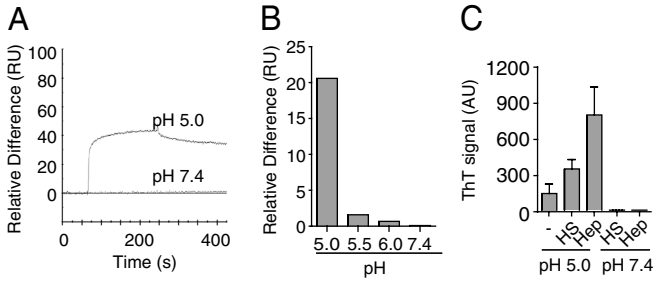

Fig. 4. HS/heparin-binding to TTR at mild acidic conditions. (*A*) Dissociated TTR was immobilized onto a Biacore sensor chip and heparin (10 μM) was allowed to interact with the immobilized TTR in neutral or in mildly acidic conditions. (*B*) HS II (10 μM) binding to TTR at different pH was monitored, and the response for each sample is expressed as response units (RU). The experiment was repeated three times, and the graph shows a representative result. (*C*) TTR (50 μM) incubated with heparin or HS II for 7 d at pH 5.0 or pH 7.4 was analyzed by ThT fluorescence. Data represent triplicate experiments (means ± SEM).

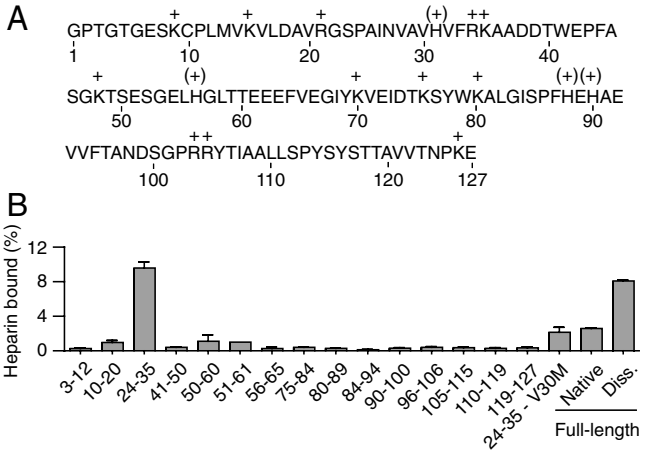

Fig. 5. Identification of HS/heparin-binding sequence in TTR. (*A*) TTR amino acid sequence where histidine "(+)" and other basic amino acids "+" are marked. (*B*) Equal mole of TTR peptides or full-length protein (with or without acidic dissociation) were incubated with ^{3}H-labeled heparin (1500 cpm) at pH 5.0. The amount of ^{3}H-labeled heparin bound to the peptides was analyzed using a nitrocellulose-filter trapping method.

To evaluate the effect of heparin on TTR fibrillization in vivo, we employed a transgenic *Drosophila* model that expresses an engineered mutant form of human TTR (16, 20). The transgenic flies were reared on standard media supplemented with or without heparin or low molecular weight heparin (Klexane©). ThT fluorescence analysis of the fly head lysate extracted in saline (see *Materials and Methods*) showed that flies fed with heparin supplement generated ThT-positive amyloid-like fibrils, whereas flies given no additive or Klexane© did not generate any fibrils (Fig. S7*A*). To corroborate the observation of substantial fibril formation in the fly head fed with heparin, the head lysate was analyzed by dot-blot stained with Alcian blue (Fig. S7*B*). Strong staining in the head lysate from flies fed with heparin was observed, whereas no staining was detected in the corresponding samples from control or Klexane-fed flies. Immunohistostaining of sections prepared from the head of TTR-transgenic flies cultured on heparin-supplemented medium revealed TTR and heparin costaining in the retina (Fig. 6*D*; a 3D view of TTR and heparin codeposited material is shown in Fig. 6*E*). Neither sections prepared from transgenic flies reared on regular medium (Fig. 6*F*), nor sections prepared from nontransgenic flies reared on heparin-supplemented medium (Fig. 6*G*), showed costaining for TTR and heparin in the retina.

Discussion

Heparan sulfate proteoglycans (HSPGs) have been identified as a codeposited component of amyloid in a number of amyloidogenic diseases (12, 13, 21, 22), and are believed to play a part in the pathology of amyloidogenesis. In this study, our primary question was whether HS is associated with TTR amyloidosis, and if so, what are the potential roles of the polysaccharide in TTR aggregation and amyloidosis?

Immunohistological examination of a heart specimen from a patient diagnosed with amyloid cardiomyopathy revealed substantial HS accumulation with TTR amyloid deposits (Fig. 1), although some of the TTR positive signals, largely in vessel walls, did not overlap with HS. This finding of a high degree of HS–TTR colocalization prompted us to explore the potential functions of HS in TTR amyloidosis. To address this question,

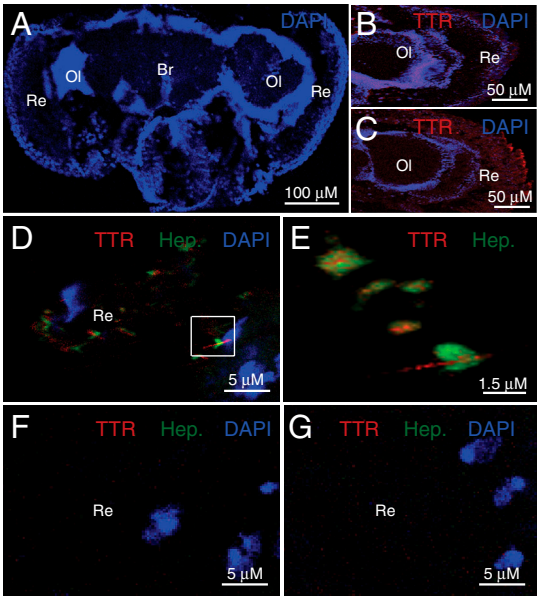

Fig. 6. Detection of heparin–TTR colocalization in TTR-transgenic flies (*A*–*G*) Confocal microscopy analysis of cryosections prepared from *Drosophila* heads. (*A*) Overview image of a *Drosophila* head stained with DAPI (blue), showing the brain (Br), optical lobes (Ol), and retina (Re). Sections prepared from transgenic flies cultured on standard medium (*B*) or heparin-supplemented medium (*C*) were stained with anti-TTR antibodies (red). (*D*) Section prepared from a transgenic fly cultured on heparin-supplemented medium was stained with antibodies against TTR (red) and heparin (green). Codeposition of TTR and heparin were observed in the retina. (*E*) An enlarged 3D view generated by a *z* stack from the marked area in *D*, showing merged staining of TTR and heparin. (*F*) Staining for TTR and heparin in a section prepared from transgenic flies reared on regular medium and (*G*) a section from non-transgenic flies fed on heparin-supplemented medium. Original magnifications, (*A*) 10×; (*B* and *C*) 20×; (*D*–*G*) 63×. Scale bars are indicated.

we employed recombinant human WT TTR to assess its aggregation in the absence or presence of heparin/HS by in vitro and in vivo experiments.

It has been established that TTR aggregation/amyloidosis is initiated by dissociation of the native tetramers, generating unstable monomers that spontaneously form oligmers (23, 24). In agreement with earlier reports (25), we confirmed dissociation of the recombinant WT TTR upon incubation at pH 2.7, as analyzed by gel electrophoresis. Formation of amyloid-like fibrils was quantified by ThT fluorescence staining, and the formation of oligomers was assessed by native PAGE. We found that the WT TTR spontaneously aggregated to some extent upon incubation at 37 °C for 48 h at pH 2.7, but not at higher pH (Fig. S1). However, prolonged incubation under mildly acidic conditions resulted in aggregation of the TTR (Fig. 4*C*), indicating altered kinetics of TTR aggregation at different pH conditions. This may reflect the in vivo situation, where repeated shortage of oxygen supply in a cardiomyopathic heart provides an acidified environment (26) that may facilitate TTR aggregation.

Addition of heparin, a commonly used analogue of HS, greatly promoted TTR fibrillization at pH 2.7 and 5.0 (Figs. 2*A* and 4*C*). Notably, inclusion of heparin resulted in a differential pattern of TTR aggregates as demonstrated by native-PAGE analysis. Substantial quantities of macromolecules remained at the top of the gel reflecting a reduction or absence of oligomeric species (Fig. 2*C*). It is possible that heparin altered the rate of monomer/oligomer fibril assembly, or redirects the aggregation pathway.

The finding that heparin is incorporated into the TTR fibrils (Fig. 3) suggests that HS/heparin can play a scaffold role, "collecting" misfolded TTR monomers and being incorporated into the fibrils. This may reflect the in vivo TTR–HS aggregation where HS on the cell surface or in the extracellular matrix functions as a scaffold/catalyst to promote accumulation and aggregation of the unfolded TTR monomers. The scheme in Fig. 7 illustrates this hypothesis of HS-mediated TTR fibrillization.

HS also promoted TTR fibrillogenesis, but to a lower degree compared to heparin (Fig. 2 *A* and *B*), in agreement with a recent report (27). Interestingly, the promoting ability of HS is associated with degree of sulfation. HS I that contains 5% trisulfated disaccharides had a marginal effect on TTR aggregation, whereas the highly sulfated HS II, containing 45% of the trisulfated component, had a stronger effect on TTR aggregation. A comparison of the TTR binding to heparin or the two HS preparations revealed that the difference in affinity was correlated with sulfation degree. TTR displayed a 10-fold higher affinity for heparin when compared to HS II and more than a 1,000-fold higher affinity when compared to low sulfated HS I (Fig. S3). However, chondroitin sulfate fails to promote aggregation of amyloid peptides, suggesting that the fine structure of HS is also important for the effect (13).

Intriguingly, the degree of HS sulfation has been reported to be age-dependent, as HS in the aorta of elderly individuals was found to be more sulfated than HS from young subjects (28). Concomitantly, aortic deposition of amyloid was found in all investigated subjects above 80 y of age (29). This may suggest an association of age-dependent alteration in HS sulfation with aortic amyloidosis. Whether the high incidence of WT TTR amyloidosis in the heart of elderly (9) is associated with a similar alteration of HS structure remains to be determined.

A long-asked question is why WT TTR forms amyloid, despite its well-demonstrated thermodynamic stability (24). To this end, our results showing that the sequence of aa 24-35 in WT TTR binds effectively to heparin may offer an explanation. In the native form of TTR, this peptide is cryptic (Fig. S8) and incapable of interacting with HS. When the protein is dissociated, the sequence becomes exposed, facilitating the interaction with HS. The basic property of the peptide, having three basic amino acids in close proximity (31-HVFRK-35), accommodates binding to the negatively charged HS/heparin through electrostatic interaction (30). This is of interest because similar HS/heparin-binding motifs have been identified for other amyloid peptides, such as amyloid-beta (13-HHQK-16) and serum amyloid A (SAA) (34-KYFHARGN-41) (31, 32).

Moreover, our finding that heparin binds better to the WT peptide (aa 24-35) than to the corresponding peptide containing

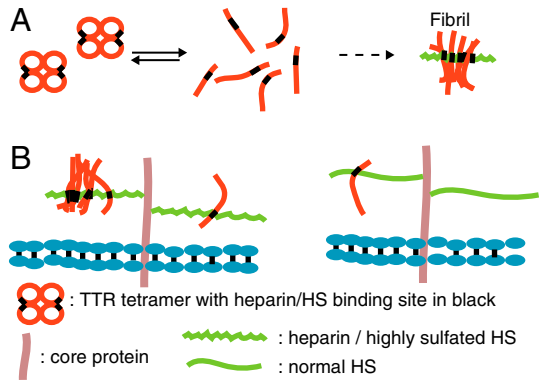

Fig. 7. Illustration of the effect of heparin/HS on TTR aggregation. (*A*) Tetramer destabilization (promoted by acidic condition) leads to formation of monomers on which the heparin/HS-binding domain is exposed. Mild acidic condition facilitates TTR binding to heparin providing a scaffold to promote fibril formation. (*B*) A hypothetical mechanism of TTR amyloidosis in the cardiac tissues. Possible change (increase of sulfation degree) in HS structure in the aged heart (*Left*) in comparison to the normal HS structure in younger individuals (*Right*) may promote TTR–HS interactions, leading to the accumulation and deposition of TTR in the heart associated with aging.

the V30M mutation (associated with familial amyloid polyneuropathy) (Fig. 5*B*) may suggest a potential mechanism for the so-far poorly understood phenomenon that V30M mutant and WT TTR display a difference in tissue-specific deposition (33). Whether this different deposition pattern is correlated to the HS-binding property of WT vs. mutant TTR should be further investigated. Examination of HS structures from the amyloid deposits of WT and V30M TTR could be valuable to establish a correlation of TTR deposition with tissue-specific HS expression.

Furthermore, we wanted to know whether the effect of HS/heparin on TTR fibrillization could be reproduced in a cell model. Incubation of the TTR with WT CHO cells that express HS (34) generated substantial amounts of amyloid-like fibrils; in comparison, the HS-deficient CHO-pgsD-677 cells only produced minor amounts of fibrils (Fig. S6). This result, combined with the strong TTR immunostaining in CHO-WT cells, clearly demonstrates a potential role for cellular HS in TTR fibrillization. This effect was further demonstrated in a *Drosophila* model that expresses an amyloidogenic TTR (16). Feeding the animals with heparin promoted formation of TTR amyloid-like fibrils, a result not observed in the flies fed with heparin fragments (Klexane®). Correspondingly, immunohistostaining with antibodies against TTR and HS confirmed the codeposition of TTR and heparin.

It should be noted that the 18-mer heparin fragment (M_r of 4,500 Da) promoted the in vitro TTR aggregation better than full-length heparin (Fig. 2*A*), whereas Klexane® (with an average M_r of 4,500 Da) failed to promote TTR fibrillization in vivo. This apparent discrepancy may be due to the molecular heterogeneity of Klexane®. The smaller fragments in the preparation may have interfered with TTR aggregation in the fly model; whereas the heparin 18-mer used in in vitro experiment is a homogenous preparation. In fact, low molecular weight heparin and heparin-like fragments have previously been shown to inhibit amyloidogenesis of SAA (35, 36) and amyloid-beta peptide (37, 38). This raises the possibility that an optimal size of heparin will be able to interfere with the TTR–HS interaction, and attenuate TTR aggregation. However, more studies are needed to clarify this possibility.

In summary, information about proamyloidogenic factors in WT TTR fibrillization is scarce. As the majority of TTR-related amyloidosis is represented by sporadic cases caused by WT TTR deposition, understanding the pathologic mechanisms of WT TTR deposition is of value for prevention and treatment of SSA. Our data provide evidence of codeposition of HS with WT TTR in a cardiomyopathic heart and illustrate a proamyloidogenic role for HS/heparin in TTR aggregation through selective binding to a specific domain of TTR. The results suggest a potential mechanism by which HS influences TTR aggregation/amyloidosis in the heart of the elderly population. The findings are consistent with reports involving other amyloid precursors, and collectively may assist in the design of potential therapeutic agents for amyloid associated diseases.

Materials and Methods

Reagents. Heparin was purchased from Kabivitrum AB. HS was isolated from porcine tissues. HS I contained 5% of the trisulfated disaccharide (IdoA2S—GlcNS6S) species and HS II contained 45% of the species. ^{3}H-labled heparin was prepared by *N*-deacetylation of the heparin followed by re-*N*-acetylation with *N*-[^{3}H]acetic anhydride. Recombinant WT TTR was used, and peptides were purchased from United Peptide Corporation or produced by G. Engström (Ludwig Institute, Uppsala, Sweden).

TTR Aggregation. For in vitro aggregation, TTR was dissolved in phosphate buffer-citric acid and heparin (^{3}H-labled or unlabeled) and HS were added to the solution. For in cell aggregation, WT Chinese hamster ovary (CHO-WT) and HS-deficient CHO-pgsD-677 (19) cells were cultured in F12 medium in the presence of 5 μM TTR for 48 h. Thereafter, the cells were extensively washed and lysed, and ThT fluorescence was measured in the supernatants. For in vivo aggregation, eggs of transgenic *Drosophila melanogaster* strain (Dhet TTR-A), generated as described (16), were reared with the standard food supplemented with or without heparin or low molecular weight heparin (Klexane®). After 10–17 d, the heads were dissected for preparation of homogenization or cryostat sections that were analyzed for TTR and heparin deposition.

Detection of TTR Aggregates. For detection of TTR–HS codeposition, the human cardiac tissue sections were stained with Congo red, sulfated Alcian blue, and immumostaining with anti-TTR and anti-HS antibodies. For fluorescent detection, sections were incubated with the relevant secondary antibodies in blocking solution. Images were captured with microscopes from Carl Zeiss. For detection of aggregation, Thioflavin T fluorescence assay or 10% native PAGE were applied.

TTR–HS/Heparin Interaction. Binding of TTR or peptides to heparin/HS was evaluated using a Biosensor system (Biacore2000) by immobilization of the protein or heparin to the chips. Alternatively, a filter-binding assay (18) was used after incubation of the protein with ^{3}H-heparin.

ACKNOWLEDGMENTS. We thank Prof. U. Lindahl (Uppsala University) for valuable scientific discussions. This work was supported by grants from the European Commission (EURAMY, European rare amyloidosis network), the Swedish Research Council (K2009-67X-21128-01-3, 5961, and 10371), the Mizutani Foundation for glycoscience, Cancerfonden (09 0717), Polysackaridforskning Foundation (Uppsala), and Föreningen mot familjär amyloidos (FAMY).

1. Blake CC, Geisow MJ, Oatley SJ, Rerat B, Rerat C (1978) Structure of prealbumin: Secondary, tertiary and quaternary interactions determined by Fourier refinement at 1.8 A. *J Mol Biol* 121:339–356.
2. Prapunpoj P, Leelawatwattana L (2009) Evolutionary changes to transthyretin: Structure-function relationships. *FEBS J* 276:5330–5341.
3. Raz A, Shiratori T, Goodman DS (1970) Studies on the protein-protein and protein-ligand interactions involved in retinol transport in plasma. *J Biol Chem* 245:1903–1912.
4. Saraiva MJ, Birken S, Costa PP, Goodman DS (1984) Amyloid fibril protein in familial amyloidotic polyneuropathy, Portuguese type. Definition of molecular abnormality in transthyretin (prealbumin). *J Clin Invest* 74:104–119.
5. Saraiva MJ, et al. (1990) Cardiac amyloidosis: Report of a patient heterozygous for the transthyretin isoleucine 122 variant. *Scand J Immunol* 32:341–346.
6. Buxbaum J, Koziol J, Connors LH (2008) Serum transthyretin levels in senile systemic amyloidosis: Effects of age, gender and ethnicity. *Amyloid* 15:255–261.
7. Cornwell GG, 3rd, Sletten K, Johansson B, Westermark P (1988) Evidence that the amyloid fibril protein in senile systemic amyloidosis is derived from normal prealbumin. *Biochem Biophys Res Commun* 154:648–653.
8. Wright JR, Calkins E (1975) Amyloid in the aged heart: Frequency and clinical significance. *J Am Geriatr Soc* 23:97–103.
9. Westermark P, Sletten K, Johansson B, Cornwell GG, 3rd (1990) Fibril in senile systemic amyloidosis is derived from normal transthyretin. *Proc Natl Acad Sci USA* 87:2843–2845.
10. Connors LH, Lim A, Prokaeva T, Roskens VA, Costello CE (2003) Tabulation of human transthyretin (TTR) variants, 2003. *Amyloid* 10:160–184.
11. Buxbaum JN, Reixach N (2009) Transthyretin: The servant of many masters. *Cell Mol Life Sci* 66:3095–3101.
12. Snow AD, Willmer J, Kisilevsky R (1987) Sulfated glycosaminoglycans: A common constituent of all amyloids? *Lab Invest* 56:120–123.
13. Kisilevsky R, Ancsin JB, Szarek WA, Petanceska S (2007) Heparan sulfate as a therapeutic target in amyloidogenesis: Prospects and possible complications. *Amyloid* 14:21–32.
14. O'Callaghan P, et al. (2008) Heparan sulfate accumulation with Abeta deposits in Alzheimer's disease and Tg2576 mice is contributed by glial cells. *Brain Pathol* 18:548–561.
15. Li JP, et al. (2005) In vivo fragmentation of heparan sulfate by heparanase overexpression renders mice resistant to amyloid protein A amyloidosis. *Proc Natl Acad Sci USA* 102:6473–6477.
16. Pokrzywa M, Dacklin I, Hultmark D, Lundgren E (2007) Misfolded transthyretin causes behavioral changes in a Drosophila model for transthyretin-associated amyloidosis. *Eur J Neurosci* 26:913–924.
17. Naiki H, Higuchi K, Hosokawa M, Takeda T (1989) Fluorometric determination of amyloid fibrils in vitro using the fluorescent dye, thioflavin T1. *Anal Biochem* 177:244–249.
18. Kreuger J, Lindahl U, Jemth P (2003) Nitrocellulose filter binding to assess binding of glycosaminoglycans to proteins. *Methods Enzymol* 363:327–339.
19. Esko JD, Stewart TE, Taylor WH (1985) Animal cell mutants defective in glycosaminoglycan biosynthesis. *Proc Natl Acad Sci USA* 82:3197–3201.
20. Olofsson A, et al. (2001) Capture of a dimeric intermediate during transthyretin amyloid formation. *J Biol Chem* 276:39592–39599.
21. Watson DJ, Lander AD, Selkoe DJ (1997) Heparin-binding properties of the amyloidogenic peptides Abeta and amylin. Dependence on aggregation state and inhibition by Congo red. *J Biol Chem* 272:31617–31624.
22. van Horssen J, Wesseling P, van den Heuvel LP, de Waal RM, Verbeek MM (2003) Heparan sulphate proteoglycans in Alzheimer's disease and amyloid-related disorders. *Lancet Neurol* 2:482–492.

23. Wiseman RL, Powers ET, Kelly JW (2005) Partitioning conformational intermediates between competing refolding and aggregation pathways: Insights into transthyretin amyloid disease. *Biochemistry* 44:16612–16623.
24. Kelly JW, et al. (1997) Transthyretin quaternary and tertiary structural changes facilitate misassembly into amyloid. *Adv Protein Chem* 50:161–181.
25. Palaninathan SK, Mohamedmohaideen NN, Snee WC, Kelly JW, Sacchettini JC (2008) Structural insight into pH-induced conformational changes within the native human transthyretin tetramer. *J Mol Biol* 382:1157–1167.
26. Graham RM, et al. (2004) A unique pathway of cardiac myocyte death caused by hypoxia-acidosis. *J Exp Biol* 207:3189–3200.
27. Bourgault S, Solomon JP, Reixach N, Kelly JW (2010) Sulfated glycosaminoglycans accelerate transthyretin amyloidogenesis by quaternary structural conversion. *Biochemistry*.
28. Feyzi E, et al. (1997) Characterization of heparin and heparan sulfate domains binding to the long splice variant of platelet-derived growth factor A chain. *J Biol Chem* 272:5518–5524.
29. Cornwell GG, 3rd, Murdoch WL, Kyle RA, Westermark P, Pitkanen P (1983) Frequency and distribution of senile cardiovascular amyloid. A clinicopathologic correlation. *Am J Med* 75:618–623.
30. Kreuger J, Spillmann D, Li JP, Lindahl U (2006) Interactions between heparan sulfate and proteins: The concept of specificity. *J Cell Biol* 174:323–327.
31. Ancsin JB (2003) Amyloidogenesis: Historical and modern observations point to heparan sulfate proteoglycans as a major culprit. *Amyloid* 10:67–79.
32. Elimova E, Kisilevsky R, Ancsin JB (2009) Heparan sulfate promotes the aggregation of HDL-associated serum amyloid A: Evidence for a proamyloidogenic histidine molecular switch. *Faseb J* 23:3436–3448.
33. Hou X, Aguilar MI, Small DH Transthyretin and familial amyloidotic polyneuropathy. Recent progress in understanding the molecular mechanism of neurodegeneration. *FEBS J* 274:1637–1650.
34. Sandwall E, et al. (2007) Heparan sulfate mediates amyloid-beta internalization and cytotoxicity. *Glycobiology* 20:533–541.
35. Zhu H, Yu J, Kindy MS (2001) Inhibition of amyloidosis using low-molecular-weight heparins. *Mol Med* 7:517–522.
36. Kisilevsky R, et al. (2003) Novel glycosaminoglycan precursors as anti-amyloid agents, part III. *J Mol Neurosci* 20:291–297.
37. Leveugle B, et al. (1998) Heparin oligosaccharides that pass the blood-brain barrier inhibit beta-amyloid precursor protein secretion and heparin binding to beta-amyloid peptide. *J Neurochem* 70:736–744.
38. Kisilevsky R, et al. (1995) Arresting amyloidosis in vivo using small-molecule anionic sulphonates or sulphates: Implications for Alzheimer's disease. *Nat Med* 1:143–148.